Influence of the powders phase composition and sintering atmosphere on the structure and magnetic properties of Mn-Zn ferrites

Ruslan Kuzmin * iD, Roman Khabirov iD, Anna Mass iD, Elena Lozhkina iD

Novosibirsk State Technical University, Novosibirsk 630073, Russia
* Corresponding author: kuzmin.2010@corp.nstu.ru

Abstract

The magnetic properties of Mn-Zn ferrites depend strongly on the microstructure, chemical and phase composition. In this paper the effect of synthesis and sintering conditions on the structure, phase composition and properties of Mn-Zn ferrites is investigated. The specimens for the study were obtained by pressureless sintering. The magnetic properties were measured on a B-H analyzer. The structure was investigated by XRD and SEM. Materials with an average grain size of 2.2 μm were obtained by sintering at a temperature of 1265 °C. It was found that an increase in the synthesis temperature from 700 to 1000 °C promotes the growth of the initial magnetic permeability of these materials from 1100 to 1370. The rapid cooling of the powders synthesized at 1000 °C allows maintaining a high content of the spinel phase. In the structure of materials obtained by sintering powders with initially high spinel content at 1300 °C, grains of abnormally large size are formed. This leads to an increase in the initial permeability, magnetic induction at H_m = 1200 A/m, f = 10 kHz and magnetic losses at high frequencies (up to 500 kHz). A material with fine-grained structure was obtained by using air at the heating stage of pressureless sintering. This contributed to the reduction of magnetic losses without a significant decrease in B_m.

Key findings

- The rapid cooling of the powders synthesized at 1000 °C allows maintaining a high content of the spinel phase.
- The use of powders with an initially low ferrite content provides a fine-grained structure after pressureless sintering.
- The use of air in the heating stage of pressureless sintering reduces the magnetic losses of Mn-Zn ferrites.

1. Introduction

Manganese-zinc ferrites are soft ferrimagnetic materials with high magnetic permeability, saturation induction and relatively low magnetic losses in the frequency range up to 500 kHz [1, 2]. They are commonly used for the manufacture of cores in various electronics applications [3, 4]. Magnetic properties of ferrites strongly depend on chemical and phase composition and microstructure [5]. Mn-Zn ferrites have a spinel crystal lattice in which metal cations occupy octahedral and tetrahedral positions in the sublattices. The distribution of cations in the sublattices has a significant effect on the magnetic properties of spinel ferrites [6, 7]. Since the method of obtaining Mn-Zn ferrites is a complex multistage process, an important task is to control the processing conditions at each stage carefully. These conditions should provide a stable and homogeneous chemical composition, a uniform grain structure, minimal intragranular porosity and a high density of sintered ferrite [8, 9].

One of the limitations in the production of Mn-Zn ferrites is the instability of the spinel phase in air at temperatures below 1000 °C [10]. It is known that in these conditions there is an exchange of electrons between Mn and Fe cations. This results in a variation of the concentration of

Mn^{2+} and Fe^{2+} ions in the spinel and its distribution over octahedral and tetrahedral positions, which significantly affects the magnetic properties of the ferrite. In extreme cases, the oxidation of manganese can lead to the decomposition of spinel into non-magnetic oxides Mn_2O_3 and Fe_2O_3, which results in an undesirable reduction of the magnetic properties of ferrite [11]. To maintain phase equilibrium in the MnO-Fe_2O_3 system, sintering of Mn-Zn ferrites was carried out in an atmosphere with controlled oxygen content [12–14].

An important step in the preparation of soft ferrites is the solid-state synthesis of powder mixtures. During this heat treatment, particles with a spinel crystal lattice are formed from oxides. The phase composition of the material before sintering depends on the conditions of preliminary heat treatment, which, as a result, affects the structure and magnetic properties of the material [15].

Chen et al. in [16] found that ferrites sintered from a powder with high content of spinel phase have higher values of magnetic permeability and low magnetic losses.

The authors of [17] studied the influence of ferrite content in pressed powders on their magnetic properties and structure. When the content of spinel phase increases, the secondary maximum of permeability appears, but magnetic losses increase. The authors attribute this to the formation of an inhomogeneous coarse-grained structure. The authors of the work [18] came to the similar conclusions. According to their results, ferrites sintered from a powder with a high concentration of spinel have a wider grain size distribution, which leads to an increase in magnetic losses. When a powder containing 50 wt.% or less spinel is used for sintering, it is possible to obtain ferrites with fine-grained structure, low magnetic losses, but not inferior in terms of initial magnetic permeability and saturation induction of coarse-grained analogues. The authors of [19] came to the conclusion that powder with high content of spinel phase requires longer grinding, since the particle size increases during synthesis and solid agglomerates are formed. As a result, the surface energy and sintering activity of the powder are reduced.

The oxygen partial pressure during sintering has a significant effect on the processes of microstructure formation, phase content and cation distribution in Mn-Zn ferrites. In this respect, much attention is payed to the control of the atmosphere at the stage of soaking at maximum temperature [20–22] and cooling [14, 22–25].

In contrast to the soaking and cooling stages, less attention is paid to the heating stage during sintering. However, the kinetics of spinel phase formation, grain growth and pore healing processes also depend on the partial oxygen pressure during heating [26]. Sankarshana Murthy et al. [27] carried out vacuum heating to avoid oxidation of Mn^{2+} to Mn^{3+}, resulting in the formation of ferrite at lower temperatures, to increase the magnetic permeability and density, and to reduce losses.

It was shown in [28] that the formation of the spinel phase is completed at 800 °C when heated in an atmosphere with low oxygen partial pressure and at 1200 °C when heated in air.

The results of [29] show that ferrites sintered at 1230 °C with heating in an argon atmosphere are characterized by a smaller grain size than those heated in air.

In this study, investigations were carried out to determine the features of structure formation and magnetic properties of manganese-zinc ferrites depending on the temperature and cooling rate after synthesis as well as the atmosphere at the heating stage of sintering. It should be noted that in the literature the change in the spinel concentration in the powder after ferritization was carried out by adding initial oxide powders or by increasing the synthesis temperature. However, the effect of cooling rate after ferritization on the structure and properties of Mn-Zn ferrites has not been previously investigated.

2. Materials and Methods

Manganese-zinc ferrite $Mn_{0.7}Zn_{0.25}Fe_{2.04}O_4$ was obtained by ceramic technology. High-purity powders of Fe_2O_3 (99.5 wt.%), $MnCO_3$ (99.5 wt.%), ZnO (99.5 wt.%) were used as starting materials. 0.3 wt.% CaO was used as an additive. An aqueous suspension with 50 wt.% content of dry solids was prepared. A 2 wt.% solution of diammonium citrate was used as dispersant. Mixing was carried out in a ball mill for 5 h using stainless steel grinding media. After mixing, the suspension was dried at 100 °C and the solid-state synthesis was carried out in air atmosphere.

After synthesis, the powder was subjected to wet grinding for 10 h. After grinding, 1 wt.% PVA and 1 wt.% PEG-400 were added to the suspension and dried at 90 °C. A press powder with granule size 100–250 µm was used for pressing ring shapes (24×12×5 mm) by uniaxial pressing with a load of 35 kN. The removal of the binder was carried out in an air atmosphere at 700 °C. Pressureless sintering was carried out in a tubular vacuum furnace with dwelling at a maximum temperature of 1265–1300 °C for 3 h in air atmosphere and the heating rate of 5 °C/min. Heating was carried out in an air atmosphere or in a vacuum at a residual pressure of 100 Pa. Cooling was carried out with a stepwise reduction of air pressure.

Diffraction analysis of the powder materials after synthesis was carried out using a synchrotron radiation source. The experiments were carried out in the transmission mode. The wavelength was 0.0178 nm. The beam size was 200×200 µm². To record diffraction patterns, a flat Mar354s detector with a pixel size of 100×100 µm² and a scanning area diameter of 345 mm was used. The obtained diffraction patterns were reduced to a linear form by azimuthal integration using the Python programming language and the PyFAI (Fast Azimuthal Integration) package. Micrographic investigation of polished specimens was carried out using a Carl Zeiss EVO 50 scanning electron

microscope (SEM), and optical microscopy was carried out using a Carl Zeiss Axio Observer Z1m microscope. The apparent density and open porosity of sintered ferrites were determined by hydrostatic weighing. Before measuring the magnetic properties, a layer of material with a thickness of 500 µm was grinded from the surface of the rings. The inductance of the sintered ring cores with test winding was measured in the temperature range from –60 to +175 °C using an LCR meter. A heat-cold chamber was used to maintain the temperature. From the inductance values, the initial magnetic permeability was calculated. The magnetic induction (B_m at H_m = 1200 A/m, f = 10 kHz), amplitude permeability (μ_a) and magnetic losses (P_s) of the ferrites were measured on an AC B-H analyzer DX-2012SA (DEXINMAG).

3. Results and Discussion

Heat treatment of the powder mixtures was carried out at a temperature of 700 °C (specimen F700) or 1000 °C (specimen F1000) with slow cooling in the furnace. The obtained XRD patterns are shown in Figure 1. Analysis of the diffraction patterns shows that after annealing at 700 °C a weak reflection of the spinel phase is observed. Increasing the synthesis temperature to 1000 °C promotes an increase in the intensity of the spinel reflections. At the same time, in both materials the dominant phase is a solid solution based on α-Fe_2O_3. In addition, the angular position of spinel and α-Fe_2O_3 reflections changes with increasing ferritization temperature. This indicates a change in the lattice parameters due to the processes of formation and decomposition of solid solutions of manganese and zinc ferrites. Consequently, the ferritization temperature affects not only the phase composition of the powder, but also the chemical composition of the phases. Therefore, the obtained powder mixtures allow us to analyse the effect of the ferritization degree on the sintering process, structure and properties of materials.

Ring-shaped specimens were prepared from powders synthesised under these conditions. Sintering was carried out at a temperature of 1265 °C with heating in vacuum at a pressure of 100 Pa. The properties of the obtained materials are shown in Table 1.
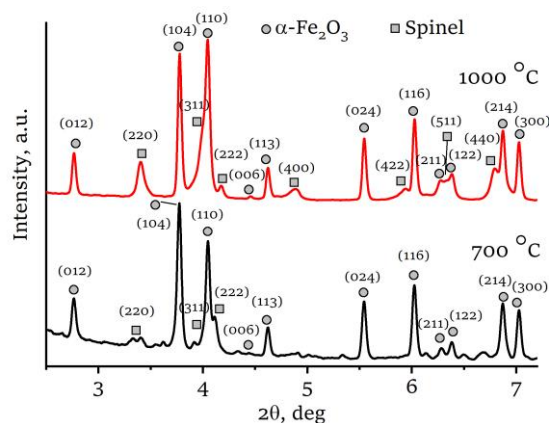
The results showed that the linear shrinkage during sintering decreases with increasing synthesis temperature. This is due to the fact that the process of ferrite formation during sintering is accompanied by a significant volumetric effect. Hence, the higher the content of ferrite phase in the material before sintering, the lower the value of shrinkage during sintering.

According to the literature [30], during the sintering of the compacts obtained from powder mixtures with a low degree of ferritization, shrinkage and ferritization processes occur simultaneously. The authors of [31] demonstrated that the specific surface area decreases with increasing synthesis temperature. A powder with a smaller specific surface area has lower surface energy and is less active during sintering, which leads to a decrease in linear shrinkage.

The structures of ferrites sintered at 1265 °C are presented in Figures 2, 3a and 3c. According to the results of SEM analysis of the materials, it was found that the structure contains large manufacturing flaws in the shape of granule boundaries.

The microstructure of the obtained materials consists of equiaxed finely dispersed grains with grain-boundary pores (Figure 3a, 3c). No intra-grain porosity is found for sintered ferrites. Figure 3b, 3d shows histograms of grain size distribution. The material obtained from the powder synthesised at 700 °C mainly consists of grains with the size from 1 to 1.5 µm.

Table 1 Properties of ferrites sintered at 1265 °C.

Properties	Synthesis temperature, °C	
	700 (F700)	1000 (F1000)
Linear shrinkage, %	18±0.3	15.8±0.2
Relative density, %	93.5±0.1	93±0.1
Open porosity, %	0.9	1.8
Average grain size, µm	1.6	2.20
Initial magnetic permeability μ_i at 25 °C	1100	1370
Maximum magnetic induction B_m, mT, (at H_m = 1200 A/m, f = 10 kHz)	444	455

Figure 1 XRD patterns of powders after synthesis at 700 and 1000 °C.
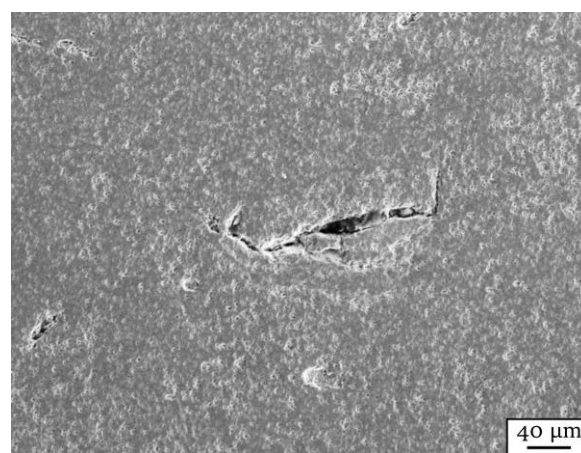
Figure 2 Common technological defects in the materials under study.
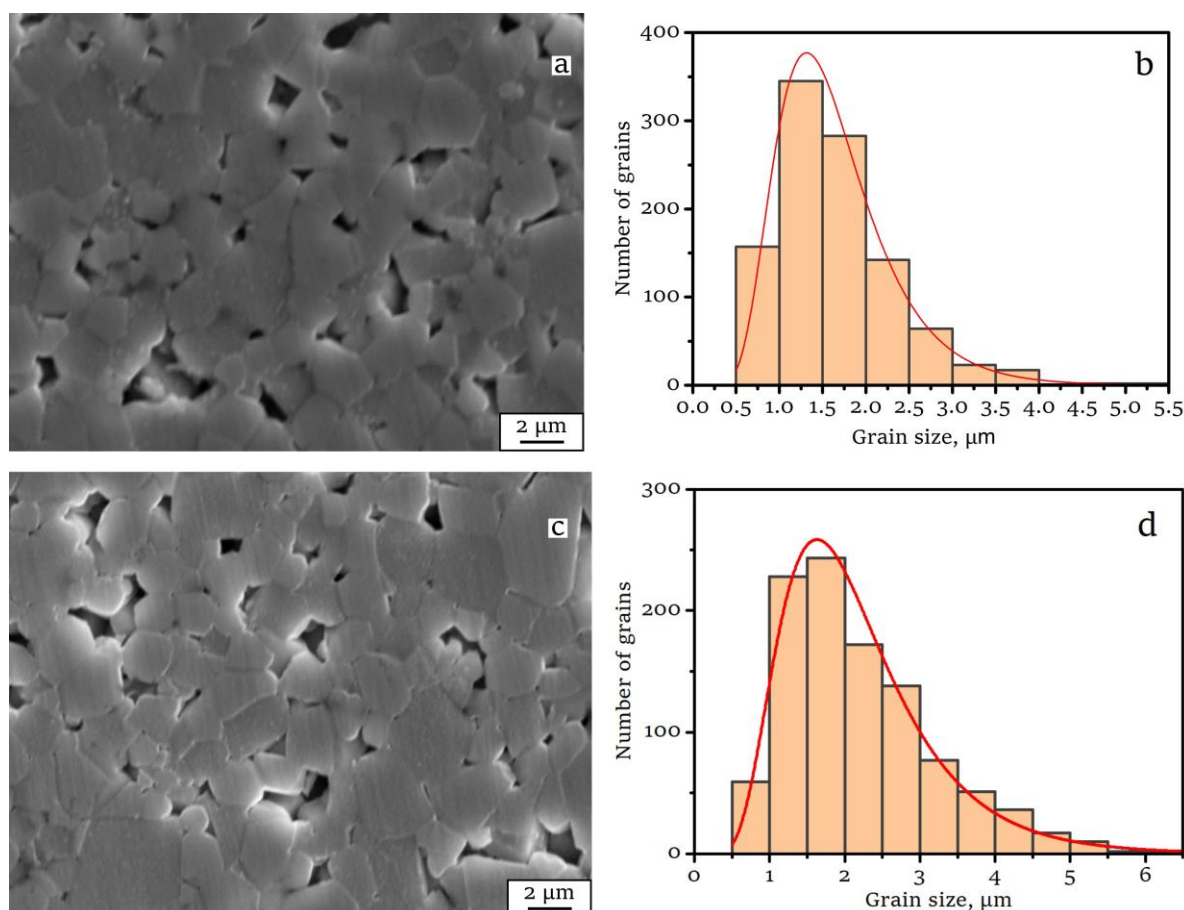
Figure 3 Microstructure of ferrites sintered at 1265 °C: microstructure of specimen F700 (a), histogram of grain size distribution of specimen F700 (b), microstructure of specimen F1000 (c), histogram of grain size distribution of specimen F1000 (d).

It was found that an increase in the synthesis temperature from 700 to 1000 °C leads to an increase in the average grain size by about 30% and an expansion of the grain size distribution. As compared to the reference data, the grain size in the obtained materials is rather small [32]. The fine-grained structure is suggested to be formed as a result of inhibition of inter-grain boundary mobility by segregated calcium cations.

An increase in the synthesis temperature from 700 to 1000 °C made it possible to improve the initial magnetic permeability μi of the sintered ferrite by 25% and the maximum magnetic induction B_m by 2.5%.

The values of the initial magnetic permeability are lower than those presented in the literature [33], which is due to the formation of a fine-grained structure.

Based on the results obtained, the synthesis temperature of 1000 °C was selected for further investigation of the influence of synthesis and sintering conditions on material properties. In order to evaluate the influence of the ferritization degree, a powder mixture synthesised at 1000 °C with air cooling was prepared. Sintering was carried out at 1300 °C to decrease porosity.

The XRD results (Figure 4) show that an increase in the cooling rate contributes to a significant increase in the intensity of the spinel phase reflections. This indicates an increase in the ferrite content in the powder after ferritization with rapid cooling.

According to the literature data [9], $MnFe_2O_4$ decomposes as a result of oxidation of Mn^{2+} cations in air at temperatures below 800 °C. Hence, the rapid cooling of the powder from the synthesis temperature helps to prevent the spinel phase decomposition. However, the XRD pattern still shows reflections of the solid solution based on α-Fe_2O_3. Consequently, the ferritization mode used does not allow obtaining a powder consisting entirely of the spinel phase. It is known [28] that spinel formation is completed in air at 1200 °C, but a decrease in the partial pressure of oxygen can lower this temperature. Thus, it is possible to obtain a powder consisting entirely of the spinel phase by increasing the ferritization temperature. However, this will lead to an increase in shrinkage and particle size of the powder, which will negatively affect sintering ability. A promising method to obtain ferrite powder consisting only of spinel can be ferritization in an atmosphere with a low oxygen partial pressure followed by rapid cooling.

An increase in the sintering temperature to 1300 °C leads to an increase in shrinkage, density, average grain size, and a decrease in open porosity (Table 2). The decrease in porosity led to an increase in the magnetic induction by 8.6% in comparison with the specimens sintered at 1265 °C. However, large flaws remain in the structure, which are attributed to incomplete destruction of the granules during pressing.
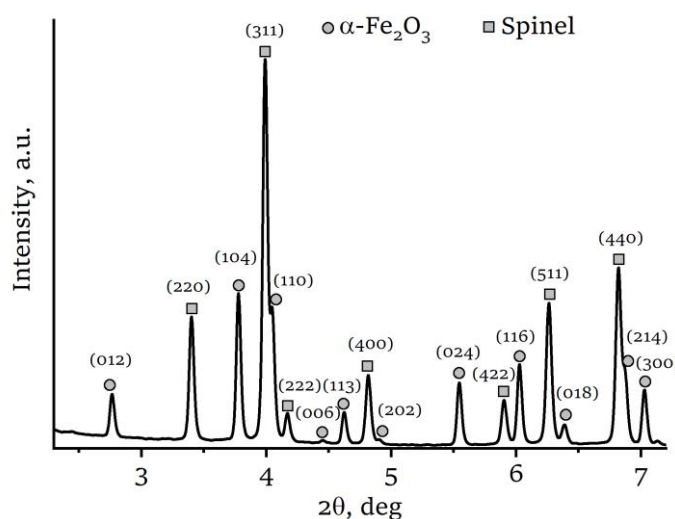
Figure 4 XRD pattern of powder after synthesis at 1000 °C and rapid cooling (F1000R).

Table 2 Properties of ferrites sintered from powder synthesised at 1000 °C.

| Properties	Synthesis conditions, °C	
	F1000, sintering at 1300 °C	F1000R, sintering at 1300 °C
Linear shrinkage, %	16.6	17.1
Relative density, %	96	94.7
Open porosity, %	0.25	0.5
Average fine grain size, μm	1.9	2.4*
Initial magnetic permeability μ_i at 25 °C	1320	1950
Maximum magnetic induction B_m, mT (at H = 1200 A/m, f = 10 kHz)	495	498

* grains with a size of 300 μm are observed.

In the surface layers of the ferrite after sintering at 1300 °C, a layer of grains with a size of 500–700 μm is formed; the structure in the middle of the specimen remains fine-grained (Figure 5). Such a feature of the microstructure change can be related to a high rate of zinc sublimation from the surface layers of the material. This process leads to an increase in the concentration of cationic vacancies, which accelerates diffusion processes and grain boundary movement [34]. The authors of [35] suggest that under sintering conditions at high temperature and low oxygen partial pressure, zinc evaporation creates micro-stresses at grain boundaries. This leads to an increase in the energy of the boundaries and an increase in its mobility.

The results of the EDX analysis of the chemical composition of the ferrite cross-section (Figure 6) show that the zinc concentration near the surface is 2 wt.% lower than in the middle of the specimen (Table 3). Thus, the formation of coarse-grained structure in the surface layers of the specimens is associated with the process of changing the chemical composition of the material.
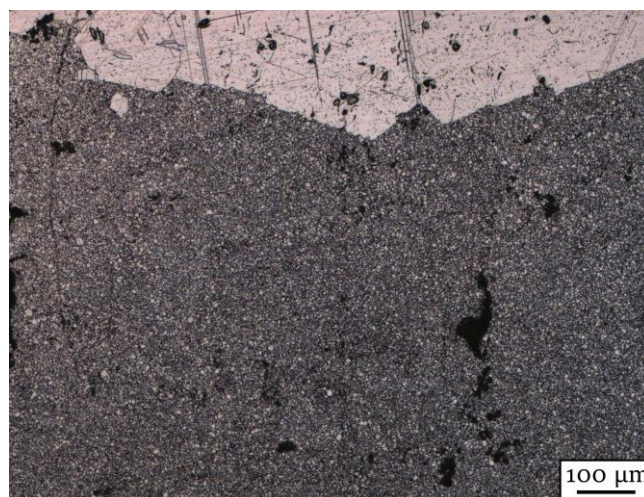
Figure 5 Coarse-grained structure in the surface layer of the material after synthesis at 1000 °C and sintering at 1300 °C with vacuum heating.
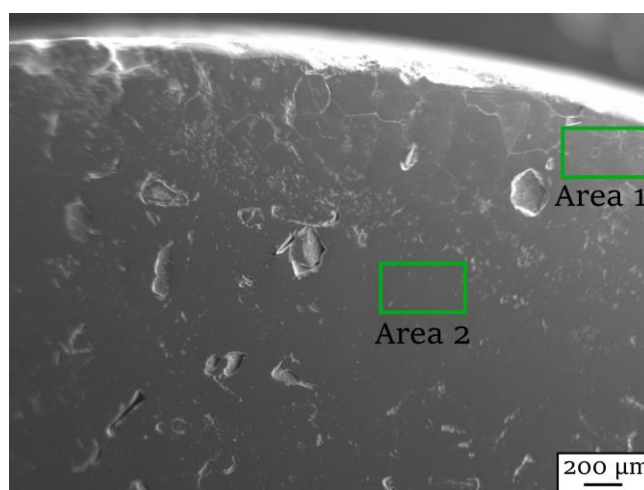
Figure 6 Cross section of sintered ferrite with marked areas for EDX analysis.

Table 3 Results of EDX analysis.

Element	Area 1, wt.%	Area 2, wt.%
Ca	0.36	0.23
Mn	22.60	20.43
Fe	67.05	67.33
Zn	9.99	12.00

It is known [36] that the intensity of zinc sublimation from Mn-Zn ferrite is inversely proportional to the partial pressure of oxygen in the furnace chamber.

In order to obtain ferrite with uniform grain size, sintering was carried out at 1300 °C, while the partial pressure of oxygen during heating was increased to the atmospheric one (0.21 atm). These sintering conditions allowed obtaining a material with uniform microstructure and an average grain size of ~1.9 μm.

Rapid cooling after synthesis had a significant effect on the microstructure of the sintered ferrites. The presence of a large amount of spinel in the powder led to the formation of abnormally large grains (the size of some grains is up to 300 μm with an average size of fine grains of 2.4 μm). It can be assumed that during the sintering process the

synthesised spinel particles had a role of secondary recrystallization sites. Meanwhile, the synthesis with rapid cooling allowed increasing the maximum induction of the sintered ferrite up to 495 mT.

An important characteristic of ferrimagnetic materials is the temperature stability of magnetic properties. In simple ferrites, the initial magnetic permeability increases monotonically with increasing temperature up to the Curie temperature. This is due to the decrease of magnetic anisotropy during heating. In spinel-type ferrites formed by solid solutions of two ferrites, magnetic anisotropy depends on temperature in a complex way. In this regard, at low temperatures, a second peak of magnetic permeability may appear, associated with a change in the sign of the magnetic anisotropy constant [37].
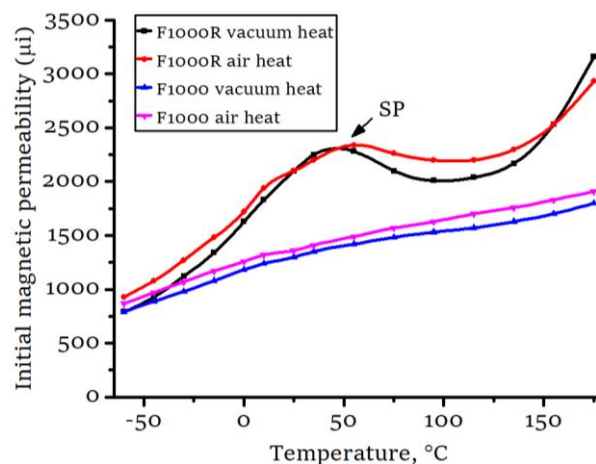
Figure 7 shows the temperature dependence of the initial magnetic permeability. In the studied materials, the most significant influence on the μ_i–T dependence is caused by the cooling rate of the powder after synthesis. The material obtained from the powder synthesised at 1000 ºC with slow cooling in the furnace is characterised by a slow increase in magnetic permeability with increasing temperature, while the synthesis with rapid cooling in air contributes to the achievement of the secondary permeability maximum. At the same time, the partial pressure of oxygen at the heating stage of sintering does not significantly affect the position and value of the secondary maximum of magnetic permeability.

The high intensity of the secondary maximum of the magnetic permeability in the samples obtained from powder with rapid cooling after synthesis can be related to the presence of abnormally large grains.

According to the literature data [38], in the equiaxed fine-grained structure of ferrites the axes of easy magnetization in single crystallites compensate each other. As a result, the polycrystalline material has a low level of magnetic anisotropy, which leads to the absence of a pronounced secondary maximum of magnetic permeability. However, in a material with significant secondary recrystallization, the easy magnetisation axes in abnormally large grains can be oriented in such a way that the magnetic anisotropy of polycrystalline ferrite is realized. This results in the appearance of a secondary maximum of magnetic permeability [39].

The values of the amplitude magnetic permeability μ_a of ferrites obtained from powders synthesised with rapid cooling are highly responsive to changes in the magnetic induction B_m (Figure 8a). The amplitude permeability increases quickly when B_m increases from 20 mT to 120 mT and then decreases. The rapid increase in magnetic permeability can be attributed to the presence of abnormally large grains in the specimen structure. Inside these grains, the domain wall movement does not require the application of a strong magnetic field; as a result, the material is easily magnetized in weak fields.

Based on the data presented in Figure 8a, it can be concluded that the increase of air pressure at the stage of heating during sintering to atmospheric one does not affect the value of magnetic induction at which the maximum values of amplitude permeability in ferrite are obtained. However, in the case of materials obtained from powders synthesised with rapid cooling, heating in air during sintering resulted in a decrease in the highest amplitude permeability by 500–600. This is probably due to the higher density and low porosity of the ferrite sintered with heating in air.

Figure 7 Temperature dependence of initial magnetic permeability for materials sintered at 1300 °C with heating under different conditions.
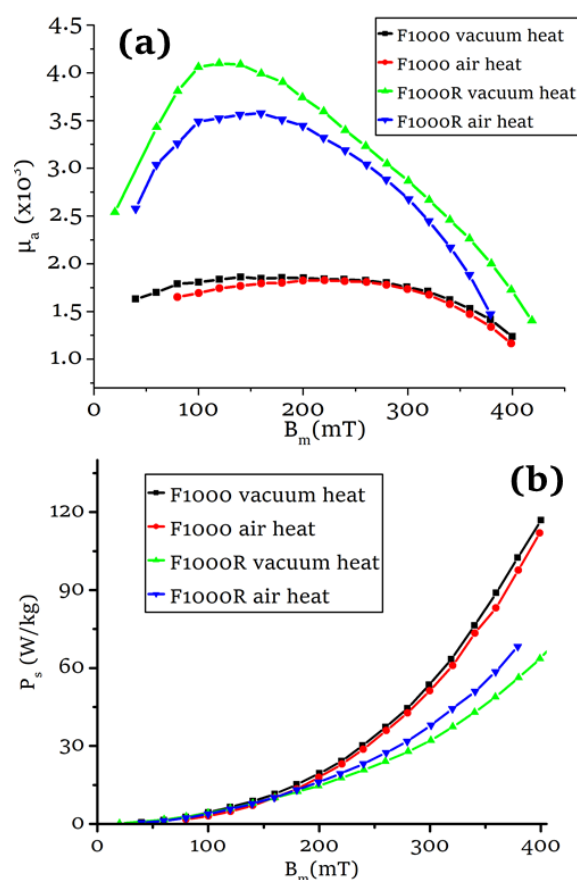
Figure 8 Amplitude magnetic permeability (a), and specific magnetic losses (b) dependence on magnetic induction (frequency 10 kHz).

With increasing temperature and cooling rate during synthesis, the magnetic losses of Ps in the ferrites decrease (Figure 9). At the applied field frequency (10 kHz) in Mn-Zn ferrites, magnetic hysteresis losses prevail, which depend on the feasibility of remagnetisation of the material, i.e., on the ease of movement of domain boundaries [40]. Hence, the presence of large grains in the ferrite structure, within which the movement of domain walls to intergranular boundaries is not difficult, can reduce the level of hysteresis losses. This can explain the low level of magnetic losses at a field frequency of 10 kHz in ferrites with signs of secondary recrystallization, i.e., those ferrites made from powders with rapid cooling after synthesis.

With increasing frequency of the applied magnetic field up to 500 kHz, eddy current losses in Mn-Zn ferrites increase. The magnitude of these losses depends on the electrical resistivity of the material. In polycrystalline ferrites, the resistivity of the grain body is significantly lower than the resistivity of the grain boundaries. In this regard, the lowest eddy current losses can be expected for the ferrites with a fine-grained crystal structure [41].

Heating in air during sintering contributed to the reduction of magnetic losses for all investigated materials (Figure 9). The combination of fine-grained structure, high level of maximum magnetic induction (485 mT at 1200 A/m, f = 10 kHz) allowed obtaining the ferrite with the lowest magnetic losses in the frequency range of 50–500 kHz at an induction of 50 mT.

4. Limitations

In this study, the solid-phase synthesis of Mn-Zn ferrites powders composed of spinel phase only was not investigated.

5. Conclusions

In this study, the influence of synthesis and pressureless sintering modes on the structure, phase composition and properties of Mn-Zn ferrites was investigated. After synthesis at temperatures of 700–1000 °C with cooling in vacuum or in air, α-Fe_2O_3 phase and spinel phase with a cubic lattice are detected in the powders. With an increase in temperature and cooling rate during synthesis, the content of spinel phase in the powder increases. It was found that the use of powder synthesised at 1000 °C with rapid cooling in air leads to the formation of abnormally large grains in the material structure. The latter causes an increase in the maximum magnetic induction up to 498 mT as well as an increase in magnetic losses at high frequencies. The use of air atmosphere during heating at the sintering stage and the formation of a fine-grained structure reduce the magnetic losses.

The lowest level of losses is observed in materials with a fine-grained structure (average grain size 1.9 μm) and high maximum magnetic induction (synthesis at 1000 °C with slow cooling, sintering with heating in air).
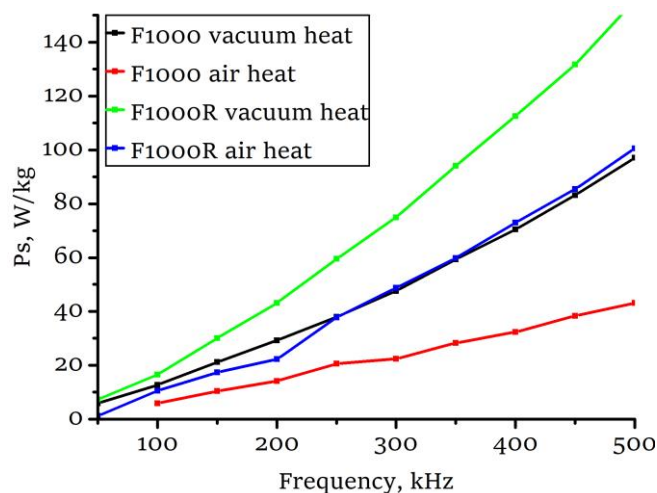
Figure 9 Frequency dependence of specific magnetic losses (B= 50 mT).

Thus, the following most important conclusions are made:

– A powder with a high spinel concentration is obtained by rapid cooling from 1000 °C.

– Rapid cooling after the calcination increases the initial magnetic permeability and decreases the magnetic losses (10 kHz frequency) in Mn-Zn ferrites.

– Pressureless sintering of ferrites from powders with a low initial spinel content promotes obtaining a fine-grained structure.

– Increasing the partial pressure of oxygen at the heating stage of pressureless sintering of Mn-Zn ferrites reduces the magnetic losses.

● Supplementary materials

No supplementary materials are available.

● Funding

● Acknowledgments

None.

● Author contributions

Conceptualization: R.K., R.Kh.
Data curation: E.L.
Investigation: R.Kh., A.M.
Methodology: R.K., R.Kh.
Validation: R.Kh.
Visualization: A.M.
Writing – original draft: R.K., R.Kh.
Writing – review & editing: E.L.

DOI: 10.15826/chimtech.2023.10.3.16

● Conflict of interest

The authors declare no conflict of interest.

● Additional information

Author IDs:

Ruslan Kuzmin, Scopus ID 57189894268;
Roman Khabirov, Scopus ID 57219412520;
Elena Lozhkina, Scopus ID 56433383400.

References

1. Zheng ZG, Zhong XC. Synthesis, structure and magnetic properties of nanocrystalline $Zn_xMn_{1-x}Fe_2O_4$ prepared by ball milling. J Alloys Compd. 2008;466(1–2):377–382. doi:10.1016/j.jallcom.2007.11.112
2. Guu YH, Tsai KL, Chen LK. An experimental study on electrical discharge machining of manganese-zinc ferrite magnetic material. Mater Manuf Process. 2007;22(1):66–70. doi:10.1080/10426910601015949
3. Sun K, Lan K, Yu Z, Xu Z, Jiang X, Wang Z, Liu Z, Luo M. Temperature and frequency characteristics of low-loss Mn-Zn ferrite in a wide temperature range. J Appl Phys. 2011;109(10):88–91. doi:10.1063/1.3583551
4. Thakur P, Chahar D, Taneja S, Bhalla N, Thakur A. A review on Mn-Zn ferrites: Synthesis, characterization and applications. Ceram Int. 2020;46(10):15740–15763. doi:10.1016/j.ceramint.2020.03.287
5. Ji X, Shen C, Zhao Y, Zheng H, Wu Q, Zhang Q, Zheng L, Zheng P, Zhang Y. Enhanced electromagnetic properties of low-temperature sintered NiCuZn ferrites by doping with Bi_2O_3. Ceram Int. 2022;48(14):20315–20323. doi:10.1016/j.ceramint.2022.03.313
6. Suryanarayana B, Ramanjaneyulu K, Raghavendra V, Murali N, Parajuli D, Mulushoa SY, Choppara P, Rao PA, Ramakrishna Y, Chandramouli K. Effect of Sm^{3+} substitution on dc electrical resistivity and magnetic properties of Ni–Co ferrites. J Indian Chem Soc. 2022;99(8):100623. doi:10.1016/j.jics.2022.100623
7. Mammo TW, Murali N, Sileshi YM, Arunamani T. Effect of Ce-substitution on structural, morphological, magnetic and DC electrical resistivity of Co-ferrite materials. Phys B Condensed Matter. 2018;531:164–170. doi:10.1016/j.physb.2017.12.049
8. Han YH, Suh JJ, Shin MS, Han SK. The effect of sintering conditions on the power loss characteristics of Mn-Zn ferrites for high frequency applications. J Phys. 1997;7(C1):111–112. doi:10.1051/jp4:1997133
9. Zhou Y, Yang G, Yang Y, Qin Y, Yin D, Zhang Y. Effect of heating rate on densification and magnetic properties of Mn-Zn ferrites sintered by multiphysical fields coupling methodology. Adv Appl Ceram. 2014;113(5):257–261. doi:10.1179/1743676113Y.0000000135
10. Goldman A. Modern Ferrite Technology. Springer Science & Business Media; 2006. 438 p.
11. Abbas T, Khan Y, Ahmad M, Anwar S. X-ray diffraction study of the cation distribution in the Mn-Zn-ferrites. Solid State Commun. 1992;82(9):701–703. doi:10.1016/0038-1098(92)90064-G
12. Morineau R, Paulus M. Chart of PO_2 versus temperature and oxidation degree for Mn-Zn ferrites in the composition range: $50<Fe_2O_3<54$; $20<MnO<35$; $11<ZnO<30$(mole%). IEEE Trans Magn. 1975;11(5):1312–1314. doi:10.1109/TMAG.1975.1058882
13. Tanaka T. Equilibrium oxygen pressures of Mn-Zn ferrites. J Am Ceram Soc. 1981;64(7):419–421. doi:10.1111/j.1151-2916.1981.tb09882.x
14. Žnidaršič A, Drofenik M. Influence of oxygen partial pressure during sintering on the power loss of Mn-Zn ferrites. IEEE Trans Magn. 1996;32(3):1941–1945. doi:10.1109/20.492890
15. Rahaman MN. Ceramic processing and sintering. CRC Press: New York; 2003. 875 p.
16. Shijie C, Science M. Effects of heating processing on microstructure and magnetic properties of Mn-Zn ferrites prepared via chemical Co-precipitation. J Wuhan Univ Technol. 2014;30(4):684–688. doi:10.1007/s11595-015-1212-8
17. Chien YT, Ko YC. Dependence of magnetic properties of Mn-Zn ferrites on the degree of calcination. J Mater Sci. 1991;26:5859–5864. doi:10.1007/BF01130125
18. Song KH, Park JH. Combined effect of partial calcination and sintering condition on low loss Mn-Zn ferrite. J Mater Sci Mater Electron. 1999;10:307–312. doi:10.1023/A:1008928903133
19. Matsuo Y, Ono K, Hashimoto T, Nakao F. Magnetic properties and mechanical strength of MnZn ferrite. IEEE Trans Magn. 2001;37(4):2369–2372. doi:10.1109/20.951175
20. Liu D, Chen X, Ying Y, Zhang L, Li W, Jiang L, Che S. Mn-Zn power ferrite with high Bs and low core loss. Ceram Int. 2016;42(7):9152–9156. doi:10.1016/j.ceramint.2016.03.005
21. Tsakaloudi V, Kogias G, Zaspalis VT. Process and material parameters towards the design of fast firing cycles for high permeability Mn-Zn ferrites. J Alloys Compd. 2014;588:222–227. doi:10.1016/j.jallcom.2013.11.047
22. Topfer J, Gablenz S. Effect of oxygen partial pressure control during sintering on the power loss in Mn-Zn ferrites. In: Proc. 9 Th Int. Conf. Ferrites (ICF 9). 2005;3:257–262.
23. Morineau R, Paulus M. Oxygen partial pressures of Mn-Zn ferrites. Phys Status Solidi. 1973;20(1):373–380. doi:10.1002/pssa.2210200139
24. Ahns SJ, Yoon CS, Yoon SG, Kim CK, Byun TY, Hong KS. Domain structure of polycrystalline Mn-Zn ferrites. Mater Sci Eng B Solid-State Mater Adv Technol. 2001;84(3):146–154. doi:10.1016/S0921-5107(00)00585-7
25. Byeon SC, Hong KS, Park JG, Kang WN. Origin of the increase in resistivity of manganese-zinc ferrite polycrystals with oxygen partial pressure. J Appl Phys. 1997;81(12):7835–7841. doi:10.1063/1.365393
26. Zlatkov BS, Mitrović NS, Nikolić M.V, Maričić AM, Danninger H, Aleksić OS, Halwax E. Properties of Mn-Zn ferrites prepared by powder injection molding technology. Mater Sci Eng B Solid-State Mater Adv Technol. 2010;175(3):217–222. doi:10.1016/j.mseb.2010.07.031
27. Sankarshana Murthy MN, Deshpande CE, Shrotri JJ. Preparation of manganous zinc ferrites. Proc Indian Acad Sci Sect A Chem Sci. 1978;87:49–54. doi:10.1007/BF03182115
28. Michalk C. Mössbauer study of Mn-Zn ferrite formation under low oxygen pressure conditions. J Magn Magn Mater. 1987;68(2):157–159. doi:10.1016/0304-8853(87)90269-1
29. Wang FFY, Krishnan KM, Cox DE, Reynolds TG. Compositional and structural studies of a Mn-Zn ferrite under different processing conditions. J Appl Phys. 1981;52(3):2436–2438. doi:10.1063/1.328959
30. Urek S, Drofenik M. Influence of iron oxide reactivity on microstructure development in Mn-Zn ferrites. J Mater Sci. 1996;31:4801–4805. doi:10.1007/BF00355864
31. Lin WH, Hwang CS. Characteristics of powder and sintered bodies of hydrothermally synthesized Mn-Zn ferrites. J Mater Sci. 2002;37(5):1067–1075. doi:10.1023/A:1014376620601
32. Stergiou CA, Zaspalis V. The role of prefiring in the development of Mn-Zn spinel ferrites for inductive power transfer. Ceram Int. 2015;41(3):4798–4804. doi:10.1016/j.ceramint.2014.12.034

33. Tsakaloudi V, Zaspalis V. Synthesis of a low loss Mn-Zn ferrite for power applications. J Magn Magn Mater. 2016;400:307–310. doi:10.1016/j.jmmm.2015.07.064

34. Yan MF, Johnson DW. Impurity-induced exaggerated grain growth in Mn-Zn Ferrites. J Am Ceram Soc. 1978;61(7–8):342–349. doi:10.1111/j.1151-2916.1978.tb09325.x

35. Sainamthip P, Amarakoon VRW. Role of zinc volatilization on the microstructure development of manganese zinc ferrites. J Am Ceram Soc. 1988;71(8):644–648. doi:10.1111/j.1151-2916.1988.tb06382.x

36. Suh JJ, Han YH. Quantitative analysis of zinc vaporization from manganese zinc ferrites. J Am Ceram Soc. 2003;86(5):765–768. doi:10.1111/j.1151-2916. 2003.tb03372.x

37. Ohta K. Magnetocrystalline Anisotropy and Magnetic Permeability of Mn-Zn-Fe Ferrites. J Phys Soc Japan. 1963;18(5):685–690. doi:10.1143/jpsj.18.685

38. Fischer R, Schrefl T, Kronmüller H, Fidler J. Grain-size dependence of remanence and coercive field of isotropic nanocrystalline composite permanent magnets. J Magn Magn Mater. 1996;153(1–2):35–49. doi:10.1016/0304-8853(95)00494-7

39. Visser EG, Johnson MT. A novel interpretation of the complex permeability in polycrystalline ferrites. J Magn Magn Mater. 1991;101(1–3)143–147. doi:10.1016/0304-8853(91)90707-H

40. Goldman A. Handbook of modern ferromagnetic materials. Springer Science & Business Media; 2012. 649 p.

41. Otsuki E, Yamada S, Otsuka T, Shoji K, Sato T. Microstructure and physical properties of Mn-Zn ferrites for high-frequency power supplies. J Appl Phys. 1991;69(8):5942–5944. doi:10.1063/1.347822